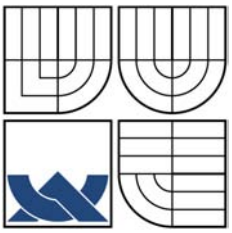

VYSOKÉ UČENÍ TECHNICKÉ V BRNĚ
BRNO UNIVERSITY OF TECHNOLOGY

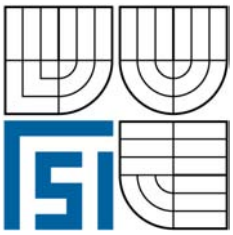

FAKULTA STROJNÍHO INŽENÝRSTVÍ
ÚSTAV FYZIKÁLNÍHO INŽENÝRSTVÍ
FACULTY OF MECHANICAL ENGINEERING
INSTITUTE OF PHYSICAL ENGINEERING

CURRENT INDUCED MAGNETIZATION DYNAMICS IN NANOSTRUCTURES

DYNAMIKA MAGNETIZACE V NANOSTRUKTURÁCH VYVOLANÁ ELEKTRICKÝM PROUDEM

ZKRÁCENÁ VERZE DIZERTAČNÍ PRÁCE
SHORT VERSION OF DOCTORAL THESIS

AUTOR PRÁCE
AUTHOR
Ing. VOJTĚCH UHLÍŘ

VEDOUCÍ PRÁCE
SUPERVISOR
prof. RNDr. TOMÁŠ ŠIKOLA, CSc.

ŠKOLITEL SPECIALISTA
CO-SUPERVISOR
STEFANIA PIZZINI, PhD.
Institut Néel, CNRS Grenoble

BRNO 2010

Klíčová slova

Přenos spinového momentu, doménová stěna, dynamika magnetizace, magnetické nanodráty, pohyb doménové stěny vyvolaný elektrickým proudem, spinový ventil.

Keywords

Spin-transfer torque, domain wall, magnetization dynamics,
magnetic nanowires, current-induced domain wall motion, spin-valve multilayers.

ISBN 80 – 214 – 1234567890
ISSN 1213 – 4198

Contents

1. Introduction

Nanotechnology has become an integral part of contemporary technology and in many fields (science, electronics, industry, medicine) it leads the innovation processes. This pursuit for improving performance of recent devices brings attention to novel fields like spintronics which upgrades the standard electronics by incorporating the spin of electrons in the electrical transport properties of materials, thus opening new horizons not only for applications, but also for enriching the basic research by investigation of mutual interaction of electrical current and magnetization.

Nowadays, magnetic materials and magnetic devices are the basic means for data storage. Hence, the findings in the spintronics field are important for applications, as they provide essential technological advances for the electronics and information technology industry. The rapidly increasing data storage capacity of harddisks is a consequence of one of the spintronics products – the giant magnetoresistance (GMR). It enabled development of harddisk read-head sensors so that they can record smaller and smaller fields of decreasing magnetic clusters where the data is stored. Since the discovery of GMR in 1988 the development has speeded up considerably, at the moment offering a large number of possible revolutionary applications in electronics. To recognize this substantial progress, the main inventers of GMR, Albert Fert and Peter Grünberg, were awarded the Nobel prize in physics in 2007.

At the end of the 1990's it was shown that a spin-polarized current excites the magnetization state and might eventually lead to the magnetization reversal. One of the most interesting consequences is the possibility to manipulate domain walls (DWs) in nanowires solely by an electric current. However, this idea is not new, the concept has been evolving since the 1950's, but it is above all the nanotechnology, in particular the lithography techniques and novel methods for observing magnetization, which gave the important impetus to the advent of investigation of current-induced domain wall motion (CIDWM). The advantage of electric current with respect to the effect of magnetic field is that it drives the domain walls in the direction of electron flow, whereas the magnetic field tends to increase or shrink domains of opposite magnetizations. This is convenient for designing magnetic storage devices based on a shift register. However, the current density required for inducing DW motion is of the order of $10^{11} - 10^{12}\,\mathrm{A/m^2}$ which justifies the need for nanowires with as small cross-sections as possible, to minimize the injected current.

The CIDWM provides a path to the design and construction of nonvolatile high-performance memories and logic systems that could take the lead over the semiconductor-based technology. However, for successful application, further optimization of systems featuring CIDWM has to be done. In particular, the critical current density has to be minimized, the DW velocity has to be maximized and to assure reproducible and reliable DW motion, pinning of DWs along the nanowire has to be controlled.

The goal of this thesis is to carry out time-resolved observation of magnetization dynamics induced by spin-polarized current. Direct imaging of CIDWM is of a high interest as it is expected to provide a key insight on the response of DW magnetization to current, allowing one to compare it to the recent theoretical predictions. The chosen system is a NiFe/Cu/Co spin-valve stack, since, as will be described in Section 3, this multilayer configuration is a promising candidate for devices based on CIDWM.

The presented manuscript summarizes the results of a joint thesis between the Institut Néel (IN) in Grenoble, France, and the Institute of Physical Engineering (IPE) at the

Brno University of Technology, Czech Republic. The author profited of the joint-thesis PhD fellowship of the French government to spend 18 months in total at the IN.

The short version of the thesis is organized as follows. As the description of theoretical background and the state-of-the-art of the spin-transfer-torque-induced DW motion is out of the range of the short version, we will just highlight the most important results we obtained. Section 1 shows one of the most interesting applications of CIDWM – the Racetrack memory. In Section 3 the most relevant papers dealing with current-induced domain-wall motion in spin-valve nanowires are summarized.

Sections 3-6 deal with the quasi-static observation of CIDWM and DW pinning. Section 7 is devoted to the time-resolved observation of magnetization dynamics in spin-valve NiFe/Cu/Co nanowires. Finally, a discussion and conclusions close the manuscript.

2. Application Concepts

Besides the fundamental investigation of the interaction of current and magnetization, the research in DW motion is motivated mainly by two applications:

- Magnetic Logic Devices
  As proposed originally by Allwood et al. [1], these devices work with field-induced DW motion. On the basis of the proposed essential logic circuits like NOT [2] and AND, any more complicated logic systems might be realized.

- Racetrack Memory
  This memory was proposed as a direct competitor to harddisks and random-access memories and has become almost a Holy Grail in the CIDWM community. The father of this idea, S. S. P. Parkin, introduced the concept of a cheap, fast, nonvolatile and low-consumption memory [3, 4]. The racetrack in Fig. 1a,b represents a nanowire with notches where the information is stored in the DWs separating domains of opposite magnetizations. Unlike magnetic field, upon applying current pulses the domain wall set moves as a whole in one direction over a read (c) and write (d) head.

  The racetrack memory does not have any rotating mechanical parts as harddisks, i.e. it is as fast as solid-state memories, but the information can be written an infinite number of times (with respect to FLASH disks which have a limited number of cell overwritings) and is preserved after the computer is powered down. The energy consumption is very low as there are no coils for production of magnetic field. The storage density is limited by the lithography state-of-the-art, in any case the 3D ordering offers a huge reserve for the expansion of the memory size (see Fig. 1e).

3. Current-Induced Domain-Wall Motion in Spin-Valve Nanowires

For spin-valve NiFe/Cu/Co nanowires, critical current densities as low as $8 \times 10^{10}\,\mathrm{A/m^2}$ were found, assuming a uniform current flow in the trilayer [5, 6]. The critical current density can be further lowered to $1 \times 10^{10}\,\mathrm{A/m^2}$ by employing CoFeB as a soft magnetic

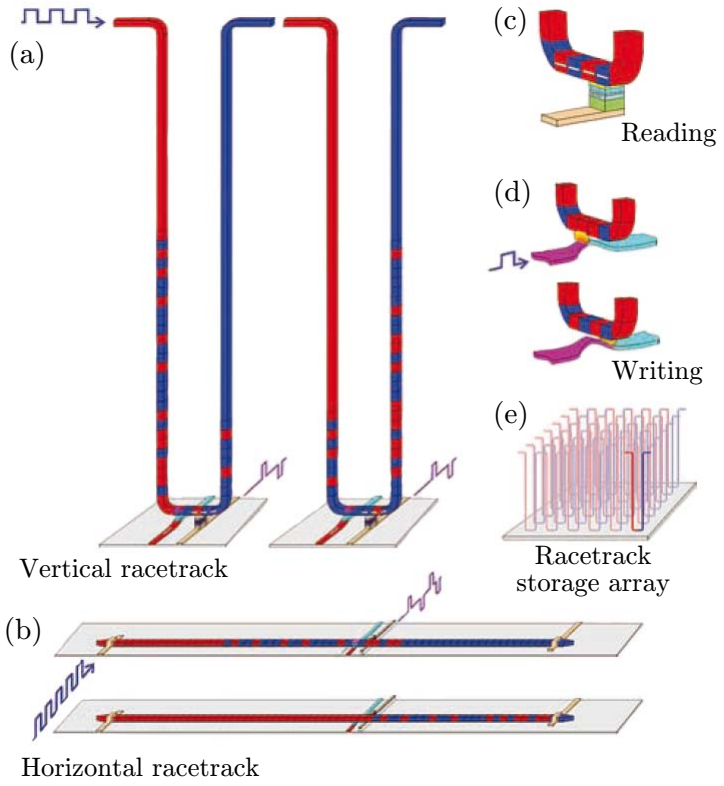

Fig. 1: The concept of the racetrack memory. (a) vertical racetrack, (b) horizontal racetrack. (c) reading data from the stored bit can be done by reading the resistance of a magnetic tunnel junction in contact with the racetrack. (d) writing of the information bit is performed by the stray field of a domain below the magnetic bit. The polarity of the "writing domain" can be altered by current injection as well. (e) concept of the racetrack array. Figure taken from [4].

layer instead of NiFe [7]. High DW velocities in this system were suggested by Lim et al. [6], who observed a 20 μm DW displacement induced by a 0.5 ns current pulse. However, besides the intriguing value of the DW velocity, many open questions arised in this work — the DW displacement did not scale with the current pulse duration and a reversal of the direction of DW motion was observed at high current densities.

We will show in Section 5 that in spin-valve nanowires DW velocities above 600 m/s and more could be achieved using relatively low current densities below 5×10^{11} A/m^2.

A theoretical work on spin injection in spin-valve systems containing DWs was carried out by Khvalkovskiy et al. [8]. They considered a spin valve system consisting of a ferromagnetic layer with a single DW, a metal spacer and a second ferromagnetic layer that is a planar (magnetization in-plane) or vertical polarizer (magnetization out-of-plane). This situation was compared to a single ferromagnetic layer. It was found that spin accumulation inside the Cu spacer layer in the region of a DW gives rise to a spin current injected vertically in the DW. This additional channel for the spin transfer from the current to the magnetic moments inside the DW might improve the spin transfer efficiency leading to a significant reduction of the critical currents. The better efficiency of spin torque has been predicted for a perfect vertical injection of the current [8]. In case of an in-plane polarizer, the DW moved at a velocity of 100 m/s at 10^{11} A/m^2.

An experimental proof of the large effect of perpendicular spin currents in spin valve systems was given by Boone et al. [9]. The authors investigated the DW motion in the NiFe layer of NiFe/Cu/$Co_{50}Fe_{50}$ spin-valve nanowires. The DW motion was driven by a resonant excitation of the DW in a potential well. Very high DW velocities of about 800 m/s at current densities as low as 9×10^{10} A/m^2 were found [9].

These advantageous results for spin-valve nanowires are very promising for the application of CIDWM. The combination of different magnetic and nonmagnetic layers might however be problematic because of a large number of free parameters to investigate [10]. Particularly the growth of the individual layers may lead to interface roughness resulting in DW pinning and the dipolar interaction between the magnetic layers is also significant. These issues were addressed in Part II of the PhD thesis manuscript.

4. Domain-Wall Observation using Photoelectron Emission Microscopy

As mentioned in the Introduction, we used the XMCD-PEEM technique for the DW observation. Details on the principle and functioning of this technique can be found in the PhD thesis manuscript. We just point out that in the presented images the black and white colors of nanowires represent opposite directions of magnetization, the gray color represents a nonmagnetic material (the substrate) or magnetization oriented perpendicular to the incidence of the x-ray beam.

Fig. 2a presents a typical NiFe multidomain magnetic configuration obtained after the application of a transverse magnetic field pulse of an amplitude not sufficient to saturate the magnetization of each zigzag section. Application of a 10-ns long pulse with a current density of 4.2×10^{11}-A/m^2 leads to a displacement of most of the DWs. As expected for spin-torque driven motion, the direction of DW motion is determined by the sense of the electron flow, as no magnetic field is applied during the current pulses. The DWs can be moved forth (Fig. 2b) and back (Fig. 2c) with opposite current polarities, unless the pinning potential is stronger in the final than in the initial position. The DW motion is not symmetric for the opposite polarities, which is often the case in our measurements, as we will show later. The average velocity of a DW can be calculated by dividing the distance traveled by a DW by the corresponding pulse duration. The average velocity of the moving DWs in Fig. 2 ranged from 130 to 240 m/s.

An apparent DW motion against the electron flow was sometimes observed. Every time that this was the case, a region with an intermediate XMCD intensity was observed at the arrival point. These regions, like the one in Fig. 2c at position B, can be due to 360° DWs smaller than our experimental resolution (see Fig. 9). A one-directional expansion of such a 360° DW upon application of a current pulse leads to an apparent domain nucleation. Such an apparent domain nucleation at position B in Fig. 2c would mean that the displacement A-C in Fig. 2b actually consists of two displacements, A-B and B-C. Such "double" displacements were not often observed and have not been taken into account in the statistical analysis of Section 5.

To prove that the DW motion is governed by spin transfer torque and not by a residual magnetic field, Fig. 3 shows head-to-head and tail-to-tail DWs moving together.

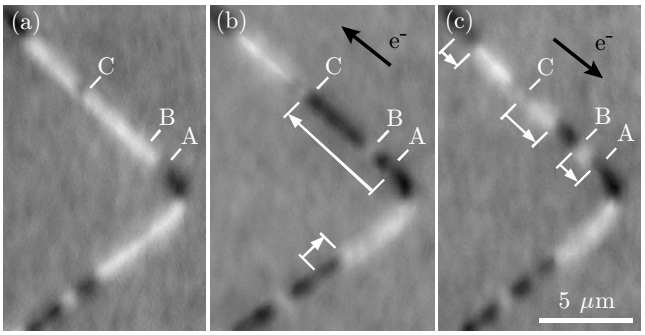

Fig. 2: Initial-state domain structure obtained for a 200 nm wide nanowire by applying a magnetic field pulse (a). DW structure obtained after the application of 10 ns long current pulses with an amplitude of 4.2×10^{11} A/m^2 with positive (b) and negative (c) polarities. The DW motion follows the direction of the electron flow. (c) Application of a negative pulse, leading to the displacement B-A, shows DW nucleation at site B.

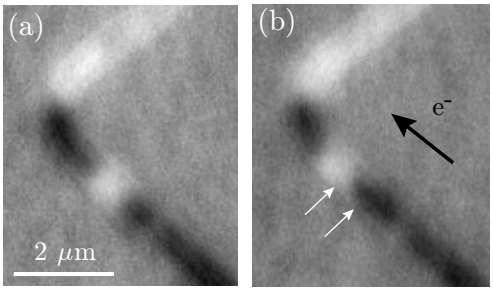

Fig. 3: (a) Initial domain structure obtained with magnetic field pulses before applying current pulses. (b) Head-to-head and tail-to-tail DWs move together upon application of a current pulse (2.5 ns, 3.3×10^{11} A/m^2). White arrows indicate the initial position of the DWs.

5. Statistics of the Current-Induced DW Motion

The XMCD-PEEM images taken after the application of a single current pulse of density $2 - 4.2 \times 10^{11}$ A/m^2 to an initial multidomain structure show that in general some DWs move, but also that many others are pinned. Taking into account only the DWs that move for a given current pulse, we have deduced DW displacement and velocity distributions for different pulse lengths and current densities (see Fig. 4-6), starting from many different initial configurations.

Note that these statistical distributions do not describe repeated displacements of the same DWs, but displacements of a multitude of DWs in different parts of the nanowire. This yields a good description of the average behavior of the system, i.e. it is not burdened by a specific pinning potential of a particular DW. DW displacements occurring between the same pinning sites multiple times were removed from the statistical file in order not to influence the distribution.

Fig. 4 shows the distributions of DW velocities obtained for a 200 nm wide nanowire using a current density of 3.3×10^{11} A/m^2 and different pulse lengths. For each pulse length, approximately 50 events were analyzed. A very large distribution of velocities is obtained, ranging from below 50 m/s to more than 600 m/s. The highest velocities could be achieved only using 3 ns long pulses. On the contrary, for very long current pulses (200 ns)

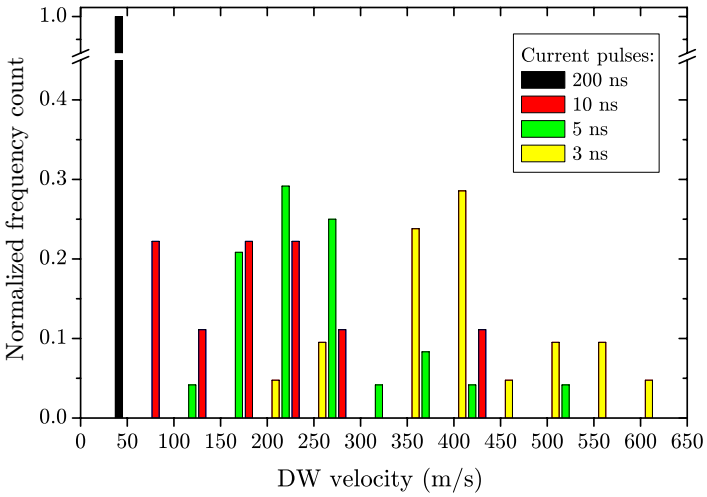

Fig. 4: DW velocity distributions obtained for a 200 nm wide nanowire using a current density of 3.3×10^{11} A/m^2 and pulse durations ranging from 3 ns to 200 ns. The computed velocities for 200-ns pulses all lie in the region below 50 m/s. The columns represent a relative number of events of a given pulse duration in the marked interval (0 50 m/s, 50 100 m/s, etc.)

only low velocities were observed. A direct comparison of the DW motion obtained with a large variety of pulse durations shows that the displacements do not scale with the pulse length and that their values are very close in general. This strongly suggests that the motion is actually limited by the positions of the pinning sites. This also explains why only by using short pulses we can provide a reliable estimate of the absolute value of the DW velocity.

In Fig. 5 we compare the integral distributions of current-induced displacements for pulse durations of 3, 5 and 10 ns - including all current density values - with the distribution of the apparent distances between potential pinning sites, identified as zones with an intermediate XMCD intensity (not shown). These distances were determined from an image of the saturated magnetic state where these zones were clearly visible. A clear correlation exists between the current-induced displacement distributions and the distances between pinning sites, confirming the influence of pinning on the DW motion.

Because of the large pinning probability, DW displacements scaling with the pulse duration were only observed in a few cases and for current pulses shorter than 12 ns. Given the values of the DW velocities and the most probable pinning site distances, it is clear that these events are unlikely: a DW propagating freely at a velocity of 400 m/s moves by 4 μm in 10 ns; as seen in Fig. 5, there are indeed very few regions of the nanowire where pinning sites are so distant. We emphasize however that the occurrence of displacements scaling with the pulse durations is an important proof that the DW moves during the current pulse and not only during the leading and falling edge of the current pulse.

In Fig. 6 we present the dependence of the DW displacement on the applied current density. Though the minimum current density for which we observed DW motion was 2×10^{11} A/m^2, only distributions obtained for higher current densities are shown. The average value of the DW displacement first shifts towards higher values as the current increases, but for the highest current values the average displacement decreases. Given the influence of pinning on the DW displacement, especially for long pulses, we emphasize that

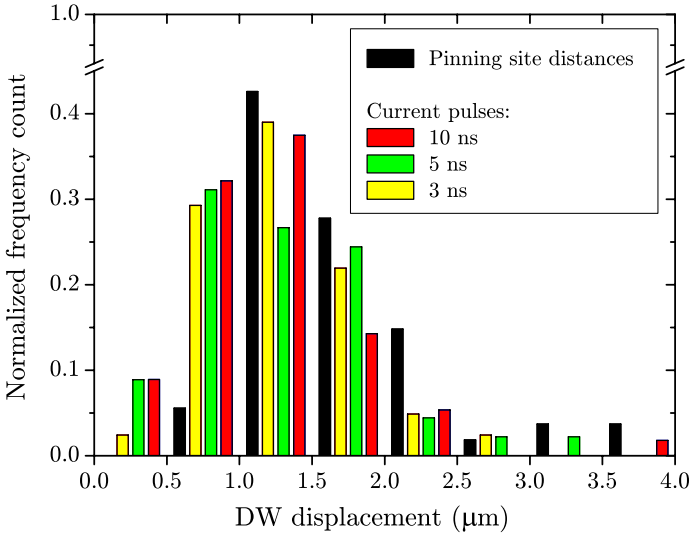

Fig. 5: Distributions of DW displacements compared to the distribution of nearest neighbor pinning site distances in a 200 nm wide nanowire, obtained for current densities in the range $2 - 4.2 \times 10^{11}$ A/m^2. For each pulse length, approx. 50 events were analyzed. The count of displacements is integrated for each marked interval. Note that the spatial resolution of our experiment did not allow determining pinning site distances smaller than 500 nm, though a relative DW displacement can be determined with a higher precision.

the shift of the displacement distributions obtained for large current densities was also present when only short pulses of 5 ns were taken into account. Note that the displacements shorter than the minimum measurable pinning site spacing (i.e. less than 500 nm, see Fig. 6) are exclusively induced by current densities higher than 4×10^{11} A/m^2. These displacements were obtained for pulse durations of 3 to 10 ns as indicated in Fig. 5.

In the inset of Fig. 6, we display the dependence of the average DW velocity on the injected current density. The DW velocity value was obtained by dividing the average DW displacement by the length of the corresponding current pulse, either 3 or 5 ns. The average DW velocity increases linearly with current density up to 4×10^{11} A/m^2. Above 4×10^{11} A/m^2, a substantial drop in the average velocity occurs. The large error bars are mainly due the widening of the displacement distributions caused by pinning.

6. Pinning of Domain Walls

Determination of Pinning Strengths

We have shown in Section 5 and 4 that the DWs can move at large velocities for relatively low current densities, as also seen in Fig. 2, but that the DW motion is strongly hampered by pinning at local defect positions. Here we support these conclusions by a systematic study showing the effect of magnetic field pulses on the multidomain structure. Fig. 7 shows the NiFe domain structure obtained after application of one 40 ns long magnetic pulse of increasing amplitude. While some DWs are unpinned by successive field pulses, a complete saturation of magnetization in the individual zigzag sections cannot be reached for the maximum field of our experimental set-up. This indicates that the pinning strength at specific positions of the nanowire is larger than 7 mT, i.e. the maximum field used here

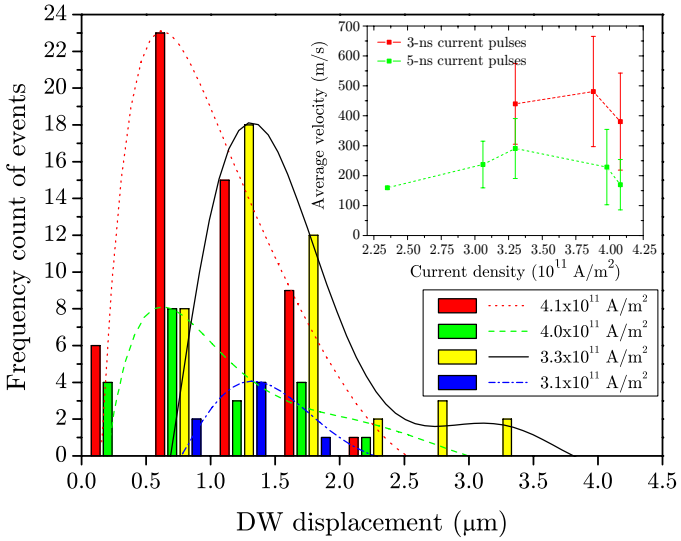

Fig. 6: DW displacement distribution in the NiFe layer, induced by current pulses of variable density. The lines are polynomial fits of the displacement distribution for a given current density and represent guides to the eye. In the inset the dependence of average DW velocity on current density is shown.

(10 mT) projected on the direction of the zigzag section. DWs are expected to be pinned at these positions also when spin-torque is the driving force for displacement.

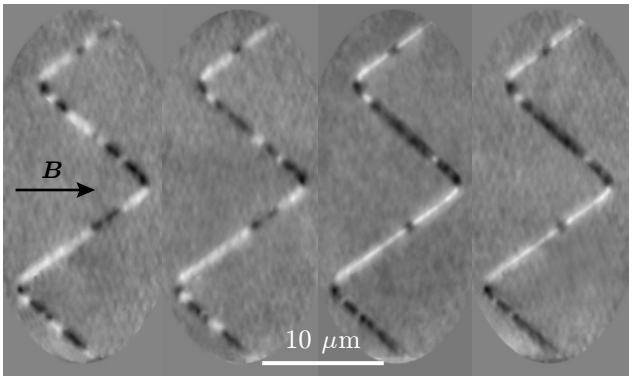

Fig. 7: Measurement of the pinning strength of DWs in a 200 nm wide nanowire. The NiFe domain structure is imaged after application of one 40 ns long magnetic pulse of increasing amplitude, going from 4 mT to 10 mT. The remaining small domains indicate the sites with the largest pinning potentials.

Possible origin of pinning

DW pinning may be induced by structural, topographic or magnetic defects. In Section 4 we showed that DWs usually stop and often get blocked for subsequent current pulses, in regions with intermediate XMCD intensities (further called "grey zones", see PhD thesis manuscript for details). These grey zones could be induced by features lowering the total x-ray absorption, like artificial defects due to the lithography process or to manipulation of the sample. We discard this possibility, since the corresponding features are generally

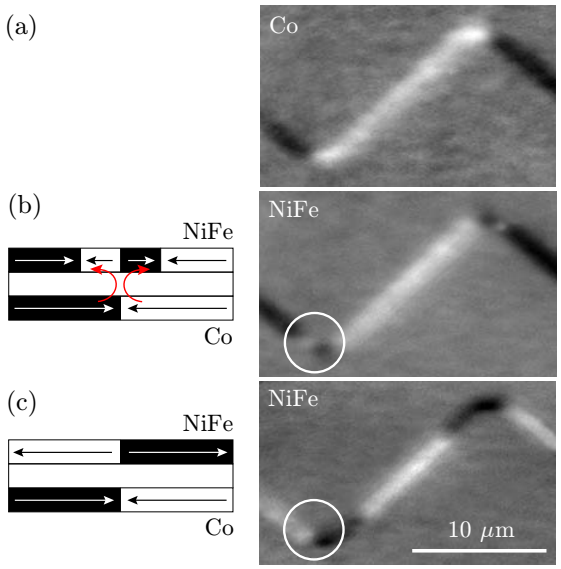

Fig. 8: XMCD images of the NiFe and Co layers of a NiFe/Cu(3nm)/Co trilayer structure, obtained after application of a strong field in the transverse direction. (a) The image taken at the Co L_3 edge shows that the DWs in the Co layer are located exclusively at the zigzag corners; in the NiFe, two kinds of domain structures can be found close to the corners, depending on whether the NiFe and Co magnetizations are parallel (b) or antiparallel (c).

absent in the sum of the images obtained for right- and left-circular polarizations. The reduced XMCD intensity is thus of magnetic origin. Since the XMCD contrast is proportional to the projection of the local magnetic moment on the incoming photon direction, a modified XMCD intensity can be caused by a tilt of the local magnetization away from the easy axis, by a reduction of the local magnetic moment or by domains (360° DWs) smaller than our spatial resolution. In the following, we discuss the different possible sources of DW pinning and their possible relation to the grey zones.

Interlayer dipolar interactions

In SV nanowires, magnetic coupling between NiFe and Co due to the orange-peel interaction associated to rough interfaces might represent a possible source of DW pinning. To check this, we have prepared specific spin-valve samples with optimized interface quality. Using ion-beam-assisted deposition with optimized deposition parameters, we succeeded in strongly decreasing the roughness of the NiFe/Cu/Co interfaces and the magnetic interlayer coupling was almost suppressed (see PhD thesis manuscript). Although the coercive field of NiFe in these samples was decreased, the grey zones were still present in the XMCD images. Interfacial roughness should thus not be at the origin of these grey zones and the associated DW pinning.

Stray fields associated with the presence of DWs or magnetic inhomogeneities in the Co layer are expected to have a strong influence on the local magnetization of the NiFe layer [10]. XMCD-PEEM measurements at the Co L_3 edge (779 eV) carried out for a NiFe/Cu/Co spin valve with a 3-nm Cu spacer (see Fig. 8a) show that DWs in the Co layer are always and exclusively located at the zigzag corners and are therefore not responsible for the modified contrast in the NiFe layer along the straight sections.

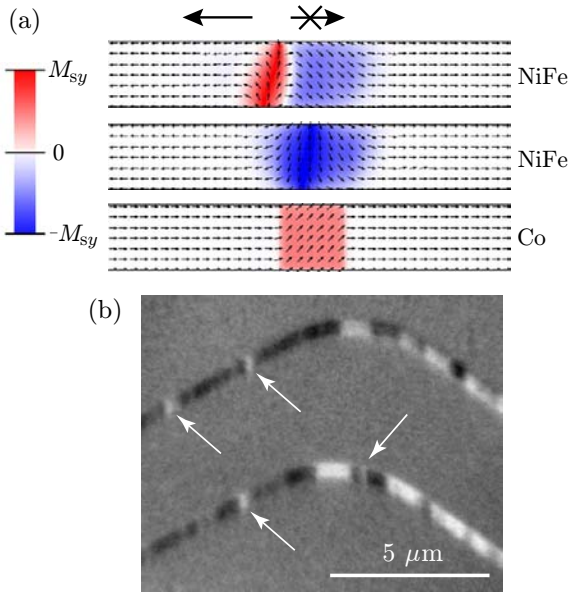

Fig. 9: (a) Micromagnetic simulations showing the effect of an anisotropy defect in the Co layer on the mobility of a DW in the NiFe layer. Each sketch represents the top view of the magnetization distribution in the Co (bottom) and NiFe layers (middle and top) under the application of a 4-mT magnetic field which drives the DW, initially in the left part of the nanowire, towards the defect. When the magnetization of the NiFe DW is in the same direction as the stray field induced by the Co defect just underneath (middle sketch) the DW is pinned at the defect position. When the Co stray field and the NiFe DW magnetization directions are antiparallel (top sketch) the DW is pushed against the region above the Co defect but cannot be moved across it. However, the DW is free to move away from the defect. (b) High resolution PEEM images of a 200 nm wide NiFe/Cu/Co nanowire. The Co images were obtained after removing part of the NiFe layer. White arrows indicate the positions of possible 360° DWs in the NiFe layer.

Note however that the stray field associated with the Co DWs strongly influences the local domain configuration in the NiFe layer. The domain structure in the NiFe layer near the corners of the zigzag provides a signature of the mutual orientation of the two ferromagnetic layers. If the Co and NiFe magnetizations are parallel, the stray field of the Co DW locally reverses the magnetization in the NiFe layer, giving rise to the three DWs shown in the white circle in Fig. 8b. If the Co and NiFe magnetizations are antiparallel, the magnetic flux closes naturally and a single DW is formed (Fig. 8c). This strong coupling prevents current-induced DW motion across the corners in the NiFe layer. This source of DW pinning can be avoided by creating a single domain in the Co layer along the nanowire.

None of the effects mentioned above seems sufficient to explain both the grey zones and the associated DW pinning. Therefore we think that these grey zones are induced by dipolar interactions between the NiFe and Co layers. These dipolar interactions will lead to a local tilt in the NiFe magnetization whenever a tilt is present in the underlaying Co layer magnetization, for instance caused by anisotropy defects. In order to verify this

scenario, we have carried out micromagnetic simulations using the OOMMF[1] code (see PhD thesis manuscript).

The stray field generated by a defect in the Co layer represents a considerable obstacle for DW motion in the NiFe layer. To illustrate this, we performed micromagnetic simulations in which a TW in the NiFe layer was driven towards the defect under the application of a 4-mT external magnetic field. If the orientation of the transverse component of the stray field and the direction of the magnetization in the NiFe DW are parallel, the DW gets pinned above the Co defect (Fig. 9a, middle). In the case of antiparallel alignment (Fig. 9a, top), the DW cannot even sit atop the Co defect, because of the high energy cost associated to the dipolar interaction. Thus, whatever the magnetization direction of the DW, a field of 4 mT cannot drive a DW across the region where the Co stray field is present. Similar effects are expected when the DW motion is induced by the electrical current.

7. Magnetization Dynamics Induced by Current

The time-resolved imaging technique was described in detail in the PhD thesis manuscript. In this Section the stroboscopic (pump-probe) set-up is exploited to investigate different aspects of the magnetization dynamics in trilayered nanowires.

Temporal resolution was obtained using the time structure of the x-ray beam at the SOLEIL synchrotron in 8-bunch mode, with a 50-60 ps long photon bunch impinging on the sample surface at a repetition rate of 6.77 MHz. Current pulses with variable lengths (2-12 ns) and amplitudes (0-10 mA) were applied to the nanowires at the same repetition rate. The temporal evolution of the magnetic configuration in the nanowires upon application of the current pulses was obtained by recording images for different delays between the current and photon pulses. The total acquisition time for each XMCD-image was about 1 minute (30 s for each circular polarisation), meaning that sequences of about 4×10^8 current (pump) and photon (probe) pulses were averaged.

By setting the delay so that the photon bunches arrive during the current pulses, we observe the instantaneous magnetization state and might obtain the DW dynamics. The effect of relatively long, 10-ns current pulses on the NiFe magnetization of a 300 nm wide nanowire is shown in Fig. 10. XMCD-PEEM images of the nanowire were taken before (a) and during the application of current pulses with amplitudes of +4 mA (b) and -4 mA (c). The corresponding current density equals to 8.9×10^{11} A/m^2 assuming a homogeneous current distribution in the stack. The electron flow direction along the nanowire is indicated in the Figure.

Before and after the current pulses, the magnetization is aligned along the nanowire and no DWs are present, leading to an almost homogeneous XMCD intensity for the NiFe layer (Fig. 10a). The contrast is slightly larger in the bends, where the magnetization is parallel to the incoming x-ray direction, than in the straight sections where the angle between magnetization direction and incoming x-rays is 45°. Surprisingly, during the current pulses, the XMCD intensity in alternate nanowire sections reverses (Fig. 10b). Importantly, after the end of the pulse, the magnetization configuration returns back to the state before the pulse. When applying pulses of opposite polarity, the XMCD intensity reverses in the sections that stayed black before. We interpreted this effect as a tilt of the

[1]Object-Oriented Micromagnetic Framework

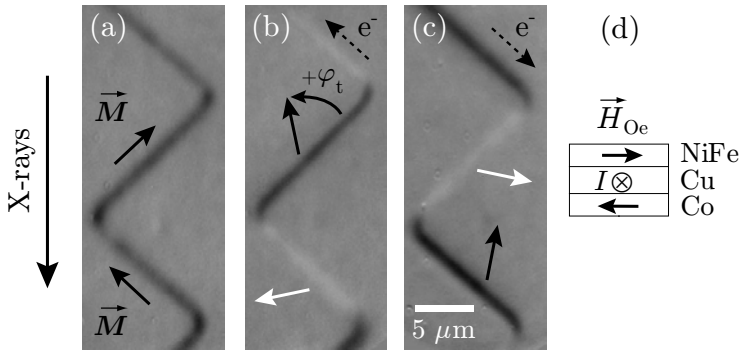

Fig. 10: Time-resolved XMCD-PEEM images of the NiFe layer of a 300 nm wide nanowire before **(a)** and during +4 mA **(b)** and -4 mA current pulses **(c)**. The arrows give the approximate magnetization direction in the nanowire, while their color gives the sign of the projection of the magnetization on the incoming x-ray direction, positive (black) or negative (white). The tilt angle φ_t, the angle between the magnetization direction and the nanowire axis, is indicated in **(b)**. The directions of H_{Oe} acting on the NiFe and Co magnetization for one current direction are schematically shown in **(d)**.

NiFe magnetization away from the nanowire axis, with a tilt angle denoted φ_t. This tilt is anti-clockwise for a positive (Fig. 10b) and clockwise (Fig. 10c) for a negative current direction. The projection of magnetization on the x-ray incidence direction changes sign for one orientation of the sections if the tilt angle exceeds 45°, as can be inferred from the magnetic contrast in the differently oriented sections of the nanowire. This is expected for a magnetization tilt induced by the Oersted field of the current in Cu and Co layers which acts on NiFe in opposite directions transverse to the nanowire for opposite current directions.

As expected, this effect takes place only in the nanowire sections where the current flows. Fig. 11 shows that during the application of a current density of 8.9×10^{11} A/m^2 the magnetization tilts only in the region in between the current contacts, while the contrast in the section below the contact, where no current flows, remains the same.

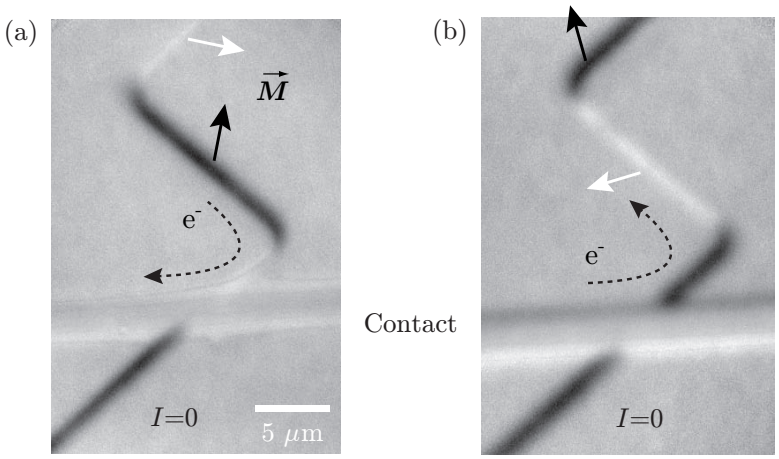

Fig. 11: XMCD-PEEM images of the NiFe layer of a 300 nm wide nanowire during the application of a current pulse of 8.9×10^{11} A/m^2. The magnetization tilts solely in between the current contacts, the bottom part stays unaffected.

The transverse Oersted field leads to a surprisingly large tilt (around 75°) of the NiFe magnetisation. For a soft magnetic material such as NiFe the magnetisation direction in a nanowire is mainly determined by magnetostatic effects, which favor magnetisation along the wire axis. For a 5 nm thick, 400 nm wide wire the transverse demagnetisation factor is about 0.023 [14], meaning that to obtain $\varphi_t = 75°$ a transverse (Oersted) field of $0.023 \times \mu_0 M_S \times \sin 75° = 22$ mT would be required (with $\mu_0 M_S = 1$ T for NiFe).

The Oersted field acting on the NiFe magnetisation, was calculated using the software package COMSOL. A current of +7 mA in the 400 nm wire, corresponding to an average current density of 1.17×10^{12} A/m^2, results in H_{Oe}= 4 mT for a homogeneous current distribution over the NiFe/Cu/Co trilayer structure, and a maximum of 6 mT for a current flowing entirely through the Cu and Co layers. This maximum value of 6 mT should lead to a magnetisation tilt φ_t of only 10° instead of the observed 75°.

An overestimation of demagnetising effect is most likely at the origin of the discrepancy between the observed and expected tilt angles. First, the transverse demagnetising factor can be smaller than the nominal value of 0.023, by several tens of percents, because of edge roughness [15], because of a decrease of effective thickness due to surface oxidation or because of intermixing at the NiFe/Cu interface. Second, the magnetostatic interaction between the NiFe and Co layers can significantly decrease the transverse demagnetising effects with respect to single NiFe wires. Part of the magnetic charges on the edges of the NiFe layer are compensated by mirroring effects on the edges of the Co layer, as has been shown by micromagnetic simulations [16]. Moreover, if the current is centered in the Cu layer the Co magnetisation tilt induced by H_{Oe} will be opposite to the one induced in the NiFe layer, further increasing the compensating effect of the Co magnetic charges. Unfortunately, the weak magnetic signal obtained for the Co L_3-edge images did not allow observing the magnetisation tilt in the Co layer during the current pulse. Finally, a larger tilt of the magnetisation at the center of the wire than at its edges is expected if one takes into account the real, non-homogeneous profile of the demagnetising field, which results from highly non-homogeneous dipolar fields in thin flat wires. The combined effect of non-uniform magnetisation in the wire, edge roughness and dipolar interactions between NiFe and Co layers can explain the large magnetisation tilt induced by H_{Oe}.

8. Discussion

In Section 7 the effect of the Oersted field was identified by time-resolved XMCD-PEEM. The Oersted field is generated by the current flowing in the Cu and Co layers of a SV nanowire and strongly affects the NiFe magnetization direction during current pulses.

Besides its influence on the quasistatic magnetic configuration in SV nanowires, we also clearly observed that the Oersted field torque affects the magnetization dynamics, by inducing a precession of the magnetization around the effective transverse field. This phenomenon might be responsible for domain nucleation above a threshold current density. This nucleation is most likely to occur at locations where a magnetization tilt in the transverse direction is already present before the current pulse, like at position B in Fig. 2c. In ref. [6], a non explained reversal of the direction of the DW motion was observed above a certain current threshold value, in SV nanowires similar to ours. Our results suggest that this effect could possibly be explained by the nucleation of a domain followed by DW motion in the direction of the electron flow, as proposed in Section 4. It is clear that a

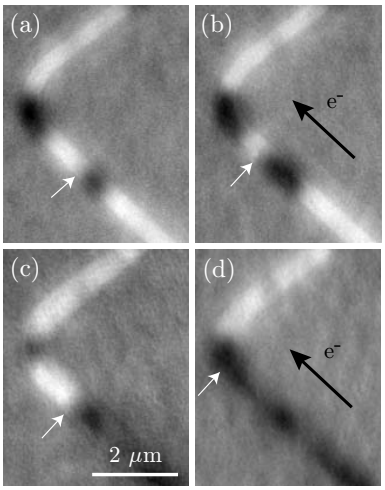

Fig. 12: Domain structures obtained: (a) before and (b) after the application of a 10-ns pulse of a current density of $4.1 \times 10^{11}\,\mathrm{A/m^2}$; (c) before and (d) after the application of a 5-ns pulse of current density $3.1 \times 10^{11}\,\mathrm{A/m^2}$. The displacement induced by the first stronger and wider pulse is shorter than that induced by the subsequent shorter pulse of lower current density. Positions of the DW are indicated by white arrows.

direct observation of the domain structure and DW motion using magnetic imaging can greatly help understanding the results obtained using magnetoresistance measurements.

An Oersted field might also modify the DW shape resulting in either a widening or a narrowing of the DW. If the DW widens, depinning becomes easier and thus might explain the lower critical current densities found for SV nanowires [5, 6, 7] with respect to single NiFe nanowires [11, 12]. The lowest current density for which DW motion was observed in our devices was $2 \times 10^{11}\,\mathrm{A/m^2}$ for the 200 nm wide nanowire. This is 3-4× lower than those published for single NiFe nanowires for similar thicknesses and widths of the NiFe layer [13]. For thicker and wider NiFe layers, a decreasing trend of critical current density has been found [12]. The actual depinning current value is determined by the strength of the individual pinning sites. In our experiments, once depinned, the DWs are able to move at high velocities, showing that we work well above the intrinsic critical density. However, because of the short pulse length and spatial resolution limitations, DW motion at very low velocities could not be detected.

Finally, we discuss the decrease of the average DW velocity observed for current densities above $4\times10^{11}\,\mathrm{A/m^2}$. This decrease could be related to the increase of the total number of DWs that are moving at high current densities, as we have observed in our images. The increased depinning probability of some strongly pinned DWs may give rise to shorter average DW displacements. This hypothesis is contradicted by the observation that some DWs that are mobile at low current densities move over a substantially shorter distance for current density above $4 \times 10^{11}\,\mathrm{A/m^2}$, as shown in Fig. 12. This suggests that the observed decrease in the DW velocity above a certain current density is real and not an artefact due to the measurement procedure or to pinning restrictions.

The impact of the Oersted field is again probably at the origin of the drop in the DW velocity observed above a certain threshold current density. On one hand, the Oersted field can stabilize the transverse walls, but on the other hand, it induces precession of the DW during its motion which might be a cause for the velocity drop above $4 \times 10^{11}\,\mathrm{A/m^2}$. The

Oersted field also leads to a widening of the DW which could result in a lower efficiency of the nonadiabatic component of the spin torque and therefore lead to lower velocities.

9. Conclusion

The presented work addressed current-induced domain wall motion in spin-valve-like NiFe/Cu/Co nanowires, using both quasi-static and time-resolved magnetic microscopy measurements. The experimental tool is the x-ray photoemission electron microscopy (PEEM) using x-ray magnetic circular dichroism (XMCD) as a source of magnetic contrast. This synchrotron-based technique combines element selectivity with a high spatial and temporal resolution.

In the quasi-static mode, domain wall displacements are obtained by the observation of the domain configuration before and after the application of one current pulse. The quasi-static measurements revealed several points. First, very high velocities for current-induced DW propagation in NiFe/Cu/Co trilayered nanowires can be found, with maximum velocities exceeding 600 m/s. The current density needed for such a rapid DW motion is of the order of 4×10^{11} A/m^2. The minimum current density for which the CIDWM was observed scales down to 1×10^{11} A/m^2 for current pulses applied to 400 nm wide nanowires and 2×10^{11} A/m^2 for both the 200 nm and 300 nm wide nanowires. The highest velocities largely exceed those found for single layer NiFe nanowires, for much larger current densities. These results show that the spin transfer torque effect is very efficient in the trilayer systems.

In quasi-static measurements, the DW velocities are deduced by the ratio of the displacement and the pulse length. The displacements do not in general scale with the pulse length. The highest presented DW velocities can be found quite rarely, as the DW motion is often stopped by pinning before the end of the current pulse. The pinning has been addressed in detail and different possible sources were carefully considered. Topography defects of whatever origin have been excluded due to the size of the pinning sites which were clearly visible as a modulation of the XMCD contrast in the images.

As no DWs in Co were present below these regions, we attributed the DW pinning to the dipolar interaction with nonuniform magnetization in the Co layer, which may be induced for instance by the crystallographic structure of Co. Micromagnetic simulations have supported this possible scenario.

The need to reduce and control pinning has speeded up the optimization of the NiFe/Cu/Co growth. We have employed Ion-Beam Assisted Deposition to modify the deposition process of this multilayer system. It was found that by assisting Ar ion bombardment of a specific energy of 50 eV, it is possible to strongly decrease the interlayer coupling so that with a 3-nm Cu spacer the NiFe and Co layers are practically decoupled. It was also observed that the use of CoO underlayers did not result in an increase of the Co coercivity, but the CoO layer prepared by oxidation during the Co deposition improved the transport properties of the system. The GMR increased up to 4.5% and the magnetization reversals became more sharp with a well defined switching field. The optimization was carried out in parallel with the XMCD-PEEM measurements during my stays in Brno, therefore the final structures could not be used before the third year of the PhD thesis.

Besides the standard e-beam lithography technique, carried out in Grenoble, the preparation of the structures by FIB has been proposed and demonstrated with the instrumentation available in Brno. The FIB-CVD technique enables one to carry out both the etching of magnetic nanowires and deposition of contacts at the same processing step. A prototype of a FIB-made structure has been made. However, FIB etching of Co layers revealed one interesting feature – although the grain size in thin Co layers is of the order of 8 nm, larger regions of grains with close crystallographic orientations, with a size comparable to the pinning sites in the XMCD-PEEM images, are present in the layers.

The second set of measurements, XMCD-PEEM in the time-resolved mode, allowed us to observe the magnetic configuration changes during the application of current pulses. The changes in the magnetic contrast are consistent with a tilt of the NiFe magnetization in the direction transverse to the nanowire direction. The Oersted field generated by the current flowing in the Cu and Co layers has been identified as the origin of the NiFe magnetization tilt.

The large tilts could not be simply explained on the basis of the analytical model for the demagnetizing fields, which predict angle about four times smaller. This discrepancy is probably due to an overestimation of the the transverse demagnetizing factor. A first origin of the decrease of the demagnetizing factor can be attributed to its inhomogeneity along the cross-section.

The effect of the Oersted field is particularly important in spin-valve systems, where the center of the current flow is expected to be situated in the highly conductive Cu spacer. The partial compensation of magnetic charges at the edges of the NiFe lines by mirroring effects in the Co layer yields larger tilts than in the single NiFe layers. This effect is further enhanced by the fact that the Oersted field acts in opposite directions on the NiFe and Co layers.

The lateral roughness of the nanowires might also substantially modify the effective demagnetizing factor by the compensation of magnetic charges at the nanowire edges.

In addition to the tilt of the NiFe magnetization, the time-resolved measurements reveal that the magnetization undergoes fast oscillations after the onset of the current pulse. These oscillations are due to the precession of the magnetization about the effective field. The presence of a random distribution of dipolar pinning sites results in an inhomogeneous magnetic contrast in the sections of the spin-valve nanowire. It turned out that the initial phase for the precessional motion is different for each of the individual oscillators. The exchange interaction between each oscillator is however such that the spatio-temporal variation of the magnetic contrast resembles that expected for spin waves.

Let us return to the high efficiency of the spin transfer in SV nanowires. There are two likely explanations for this effect. First, vertical spin currents resulting from a local spin accumulation near the DW in the Cu spacer can provide an additional channel for the spin transfer resulting in large DW velocities, as it was theoretically predicted.

Second, the presence of a surprisingly large effect of the Oersted field on the nanowire magnetization could strongly influence domain wall dynamics in NiFe. It has been shown in the literature that transverse fields stabilize one chirality of TWs during field-driven DW motion. The spin-valve system is a bit more complex, as the flux closure between a TW in the NiFe layer and a quasi-wall in the Co layer should also contribute to preventing an easy switching of the structure by the Oersted field. In any case, we expect that the DW transformations responsible for the slow and chaotic DW motion beyond the

Walker breakdown should be inhibited. This has not yet been confirmed by micromagnetic simulations.

In summary, we have shown that spin-valve nanowires are a very interesting research subject for fundamental understanding of spin torque effects in complex systems and moreover, are highly promising systems for applications to spintronic devices. The DW velocities in NiFe are 4 to 5 times larger than the maximum value reported for other in-plane anisotropy systems, where velocities in the order of 100 m/s have been published. Given the role of pinning in the NiFe/Cu/Co system and the way the velocities have been measured, we believe that the ultimate DW velocities in this kind of systems could even exceed 600 m/s. The idea is supported by intriguing preliminary results of the time-resolved DW motion where in two different measurement scenarios the DW velocity largely exceeded 1000 m/s.

High DW velocities achievable at relatively low current densities make spin-valve systems promising for spintronic devices based on DW displacement. Such trilayers are naturally much more complex than the generally used NiFe systems. We have identified the main pinning sources, among which the dipolar interaction of the NiFe layer with Co anisotropy inhomogeneities is the most probable and should be controlled in order to be able to discover the full capabilities of the system and to employ it in the future DW devices.

References

[1] D. A. Allwood, G. Xiong, C. C. Faulkner, D. Atkinson, D. Petit and R. P. Cowburn, *Magnetic domain-wall logic*, Science **309**, 1688 (2005).

[2] D. A. Allwood, G. Xiong, M. D. Cooke, C. C. Faulkner, D. Atkinson, N. Vernier and R. P. Cowburn, *Submicrometer Ferromagnetic NOT Gate and Shift Register*, Science **296**, 2003 (2002).

[3] S. S. P. Parkin, *Shiftable Magnetic Shift Register and Method of Using the Same*, U.S. Patent No. 6834005 (2004).

[4] S. S. P. Parkin, M. Hayashi and L. Thomas, *Magnetic Domain-Wall Racetrack Memory*, Science **320**, 190 (2008).

[5] J. Grollier, P. Boulenc, V. Cros, A. Hamzić, A. Vaurès, A. Fert and G. Faini, *Switching a spin valve back and forth by current-induced domain wall motion*, Appl. Phys. Lett. **83**, 509 (2003).

[6] C. K. Lim, T. Devolder, C. Chappert, J. Grollier, V. Cros, A. Vaurès, A. Fert and G. Faini, *Domain wall displacement induced by subnanosecond pulsed current*, Appl. Phys. Lett. **84**, 2820 (2004).

[7] S. Laribi, V. Cros, M. Muñoz, J. Grollier, A. Hamzić, C. Deranlot, A. Fert, E. Martínez, L. López-Díaz, L. Vila, G. Faini, S. Zoll and R. Fournel, *Reversible and irreversible current induced domain wall motion in CoFeB based spin valves stripes*, Appl. Phys. Lett. **90**, 232505 (2007).

[8] A. V. Khvalkovskiy, K. A. Zvezdin, Ya. V. Gorbunov, V. Cros, J. Grollier, A. Fert and A. K. Zvezdin, *High Domain Wall Velocities due to Spin Currents Perpendicular to the Plane*, Phys. Rev. Lett. **102**, 067206 (2009).

[9] C. Boone, J. A. Katine, M. Carey, J. R. Childress, X. Cheng and I. N. Krivorotov, *Rapid Domain Wall Motion in Permalloy Nanowires Excited by a Spin-Polarized Current Applied Perpendicular to the Nanowire*, Phys. Rev. Lett. **104**, 097203 (2010).

[10] L. Thomas and S. Parkin, *Current Induced Domain-wall Motion in Magnetic Nanowires* in *Handbook of Magnetism and Advanced Magnetic Materials*, vol. 2, eds. H. Kronmüller and S. Parkin. John Wiley & Sons, Ltd. (2007).

[11] M. Hayashi, L. Thomas, C. Rettner, R. Moriya, Y. B. Bazaliy and S. S. P. Parkin, *Current Driven Domain Wall Velocities Exceeding the Spin Angular Momentum Transfer Rate in Permalloy Nanowires*, Phys. Rev. Lett. **98**, 037204 (2007).

[12] L. Heyne, J. Rhensius, Y.-J. Cho, D. Bedau, S. Krzyk, C. Dette, H. S. Körner, J. Fischer, M. Laufenberg, D. Backes, L. J. Heyderman, L. Joly, F. Nolting, G. Tatara, H. Kohno, S. Seo, U. Rüdiger and M. Kläui, *Geometry-dependent scaling of critical current densities for current-induced domain wall motion and transformations*, Phys. Rev. B **80**, 184405 (2009).

[13] N. Vernier, D. A. Allwood, D. Atkinson, M. D. Cooke and R. P. Cowburn, *Domain wall propagation in magnetic nanowires by spin-polarized current injection*, Europhys. Lett. **65**, 526 (2004).

[14] A. Aharoni, *Demagnetizing factors for rectangular ferromagnetic prisms*, J. Appl. Phys. **83**, 3432 (1998).

[15] R. Cowburn, D. Koltsov, A. Adeyeye and M. Welland, *Lateral interface anisotropy in nanomagnets*, J. Appl. Phys. **87**, 7067 (2000).

[16] J. M. B. Ndjaka, A. Thiaville and J. Miltat, *Transverse wall dynamics in a spin valve nanostrip*, J. Appl. Phys. **105**, 023905 (2009).

Abstrakt

Předkládaná dizertační práce pojednává o problematice pohybu doménových stěn (DS) vyvolaného spinově polarizovaným proudem v magnetických nanodrátech na bázi spinového ventilu NiFe/Cu/Co. Jedná se o tzv. efekt přenosu spinového momentu. Multivrstevnatý systém NiFe/Cu/Co, kde se doménová stěna pohybuje ve vrstvě NiFe, vykazuje velmi vysokou účinnost přenosu spinového momentu, což bylo v literatuře potvrzeno na základě magnetotransportních měření.

Tato práce má za cíl pozorovat stav DS během jejich pohybu, pomocí fotoelektronové mikroskopie kombinované s kruhovým magnetickým dichroismem. Tato technika využívá synchrotronové záření, které svým časovým rozlišením umožňuje sledovat dynamickou odezvu magnetizace na elektrický proud.

Podstatnou částí řešení byla optimizace růstu vrstev NiFe/Cu/Co kvůli snížení magnetické dipolární interakce mezi vrstvami. V práci je také řešen způsob přípravy nanodrátů litografickými metodami.

Byly provedeny dva módy měření: i) kvazistatický, tj. pozorování DS před a po injekci proudu do nanodrátu a ii) dynamické měření, kde je DS sledována během působení proudového pulzu. S využitím kvazistatickém módu byla vypracována rozsáhlá statistika pohybu DS: i) byly naměřeny jejich vysoké rychlosti přesahující 600 m/s za působení průměrné proudové hustoty nutné k posuvu doménové stěny - 5×10^{11} A/m^2; ii) DS jsou v systému NiFe/Cu/Co velmi silně zachycovány dipolární interakcí mezi NiFe a Co způsobenou nehomogenitou krystalové struktury ve vrstvě Co.

V dynamickém módu bylo odhaleno, že působením Oerstedovského pole kolmého na nanodráty v rovině vzorku se magnetizace ve vrstvě NiFe silně natáčí. Tento efekt přispívá k vysokým rychlostem DS pozorovaných v nanodrátech NiFe/Cu/Co.